Surface & Coatings Technology 381 (2020) 125216

Contents lists available at ScienceDirect

Surface & Coatings Technology

journal homepage: www.elsevier.com/locate/surfcoat

On the wear and corrosion of plasma nitrided AISI H13

F.A.P. Fernandes[a,*], S.C. Heck[b], C.A. Picone[c], L.C. Casteletti[b]

[a] Centro de Engenharia, Modelagem e Ciências Sociais Aplicadas, Universidade Federal do ABC, Alameda da Universidade, s/n., 09606-045 São Bernardo do Campo, SP, Brazil

[b] Departamento de Engenharia de Materiais, Escola de Engenharia de São Carlos, Universidade de São Paulo, Av. João Dagnone, n. 1100, 13563-120 São Carlos, SP, Brazil

[c] Departamento de Física e Química, Faculdade de Engenharia de Ilha Solteira, Universidade Estadual Paulista, Av. Brasil Centro, n. 56, 15385-000 Ilha Solteira, SP, Brazil

ARTICLE INFO

Keywords:
Plasma nitriding
Tool steels
AISI H13
Wear
Corrosion

ABSTRACT

Tool steels are applied in a variety of industrial operations providing a good balance of properties. Surface engineering has the potential to improve productivity and further extend the lifetime of metallic components. In the present work plasma nitriding is applied to the hot work AISI H13 tool steel to improve wear and corrosion characteristics. The steel was nitrided in the tempered condition at three different temperatures and pressures for 5 h of duration. At 450 °C of nitriding temperature mainly a diffusion zone is observed while a compound layer is produced at 550 and 650 °C. Both surface and bulk hardness decrease as nitriding temperature is increased. X-ray diffraction indicates that a mixture of both ε and γ′ iron nitrides is produced in all cases. The content of ε-nitride appears to decrease with temperature while γ′-nitride and CrN increase. Working pressure does not lead to significant alterations in phase proportion, hardness and wear resistance after plasma nitriding at a given temperature. However, increasing processing temperature, from 450 to 650 °C, reduces the wear coefficient from $1.19 \cdot 10^{-7}$ to $7.06 \cdot 10^{-8}$ $mm^3/N{\cdot}m$, respectively, while from the base steel such coefficients are in the order of 10^{-5} $mm^3/N{\cdot}m$. Regarding the corrosion behavior, plasma nitriding at 450 and 550 °C yields higher corrosion potentials, lower current densities and an extensive passivation range, while the tempered substrate, irrespective the condition, exhibits no passivation. From the wear and corrosion perspective it is concluded that plasma nitriding at 450 or 550 °C leads to better corrosion properties while nitriding at 650 °C yields a better wear performance.

1. Introduction

AISI H13 is a chromium-molybdenum-vanadium alloyed steel and perhaps the most popular and versatile hot work tool steel widely used as a die in die-casting, extrusion and hot forging. It provides a good balance of toughness, heat resistance and temper resistance, along with moderate wear resistance. These properties can be obtained by a heat treatment process which consists of an austenitization step with a subsequent quenching and a tempering procedure [1,2]. The achieved mechanical properties are due to nanometer size alloy carbides which precipitate during tempering [1,3]. Tempering temperatures usually vary from 250 to 600 °C depending on the required characteristics for each application.

Surface engineering is a common practice in industry to improve productivity and quality further extending the lifetime of metallic components. Nitriding is a thermochemical surface treatment with a great importance because it can improve fatigue strength, tribological properties and/or corrosion resistance [4]. The process involves diffusion of nitrogen species from different types of media leading to the formation of nitrogen-rich phases in the near surface region [4].

Plasma nitriding of a variety of ferrous alloys, including tool steels, usually yields a top compound layer (or white layer) consisting of iron nitrides such as the epsilon phase (ε-$Fe_{2-3}N$), the gamma phase (γ′-Fe_4N), or a mixture of both (ε + γ′). Beneath the compound layer a diffusion zone is observed, which consists of a nitrogen interstitial solid solution in the ferrite matrix and fine, coherent nitride precipitates [5–7].

AISI H13 is particularly suitable for nitriding owing to its chromium, molybdenum and vanadium content which increase the nitrogen uptake capability [8]. Nitrogen diffusion on this steel is observed at temperatures as low as 260 °C. The ε-nitride is the first to be produced at lower temperatures while γ′-nitride precipitates at higher plasma processing temperatures [9]. Meanwhile, increasing the applied pressure leads to a reduction in case thickness due to a decrease in the mean

* Corresponding author.
E-mail address: frederico.fernandes@ufabc.edu.br (F.A.P. Fernandes).

https://doi.org/10.1016/j.surfcoat.2019.125216
Received 6 September 2019; Received in revised form 26 November 2019; Accepted 29 November 2019
Available online 30 November 2019
0257-8972/ © 2019 Elsevier B.V. All rights reserved.

free path during plasma nitriding [10,11]. Most of the articles in the literature apply nitriding temperatures no higher than 590 °C [2,5,7,9]. In the present study a nitriding temperature as high as 650 °C was chosen in order to evaluate the effects of massive nitride formation.

The composition and thickness of nitrided layers strongly depend on the processing parameters, such as treatment temperature and duration, atmosphere composition and additionally on the substrate composition. Several studies state that fatigue performance [12], tribological characteristics [13] and corrosion resistance [7] are intimately related to these characteristics of the case.

Previous research indicates that ε-nitride has a better corrosion resistance when compared to the γ′-nitride [7]. Regarding the tribological performance a study observed that a single ε-nitride layer is more wear resistant than a mixed (ε + γ′) layer at room temperature in a pin-on-disc device [14]. Other authors state that a combination of higher hardness and deeper case is adequate to reduce the extent of material loss under dry conditions [15]. Moreover, it has been reported that a γ′-nitride single layer also possesses significant ductility and lubricity [16].

Some authors have reported porosity formation in the nitrided layer upon prolonged treatments occurring as a consequence of the inherent metastability of iron nitrides [17,18]. The presence of porosity could impair the corrosion and wear properties in a given application.

Therefore, to correctly select the processing parameters for nitriding a given steel in a specific application, a proper understanding of each parameter and its effects on the microstructure and properties is relevant. In the present study the effects of plasma nitriding temperature and pressure on the microstructure, wear and corrosion properties of the AISI H13 tool steel is addressed.

2. Experimental

Initially, a square billet of AISI H13 was austenitized at a temperature of 1050 °C for 2 h followed by quenching in oil. Tempering was performed sequentially at 590 °C for a period of 2 h resulting in a bulk hardness of 770 HV (~63HRC). For the present study square samples with a side of 20 mm and thickness of 5 mm were cut from the AISI H13 heat treated billet with the following chemical composition: Fe-0.45C-0.43Mn-1.07Si-1.21V-4.60Cr-1.39Mo (wt%). The flat surfaces of the specimens were ground and polished at a final step of 1 μm alumina suspension to achieve a mirror-like surface finish.

Quenched and tempered samples were then plasma nitrided using the direct current (DC) method, applying a gas mixture of 80 vol% H_2 and 20 vol% N_2, pressure of 4, 5 and 6 mbar and temperatures of 450, 550 and 650 °C. Pressure range was selected based on previous experience knowing that values as high as 7 mbar yield an excessively thin or absent plasma sheath and values low as 2–3 mbar result in a sparse sheath. Additionally, nitriding temperatures were chosen according to an expected layer morphology. The treatments were performed in a dedicated chamber described previously [19] with a time duration of 5 h for all conditions. Plasma nitrided specimens were characterized by optical microscopy, X-ray diffraction, Vickers microhardness measurements, wear and corrosion tests.

X-ray diffraction (XRD) patterns were obtained at the surface of the samples applying a *Geigerflex Rigaku* equipment with a scanning angle from 30 to 95°. The tests were performed using copper radiation (Cu Kα) and continuous scanning with a speed of 2°/min. The patterns are plotted as a stack for each treatment temperature and relative intensities are shown. Additionally, to comparatively evaluate the phase evolution from 450 to 650 °Ca qualitative plot is given based on the absolute intensities of selected peak positions from distinct compounds, namely αFe, Fe_3N, Fe_4N and CrN. The plot was constructed by taking the average of the absolute intensities from the three different applied pressures for each compound and nitriding temperature.

For metallographic investigation, cross sections of the plasma nitrided samples were hot mounted, followed by grinding and polishing. Optical microscopy observation was conducted in a *Zeiss* microscope *Axiotech* model after etching the specimens with a 10% Nital solution. *Vickers* microhardness measurements were performed on the mounted cross sections using a digital *Buehler* equipment model *Micromet 2104* applying 100 gf of load and a dwell time of 10 s. Microhardness profiles were obtained by systematically measuring hardness on the etched cross sections from the near surface region towards the bulk. A linear sequence of indentations was performed at approximately 45° from the surface until a constant value is observed. The distance between the measurements was at least three times the size of an indentation.

A micro-abrasive wear machine was applied for studying the wear resistance of treated and untreated systems. Tests were performed in a fixed ball machine (described elsewhere [20]) without abrasive and using a AISI 52100 steel sphere of 25.4 mm in diameter as a counterbody with hardness of approximately 850 HV. The rotation speed and load were 500 rpm and 250 g (2.5 N), respectively. Consecutive wear scars were produced for test times of 5, 10, 15, and 20 min in order to obtain the volume loss curve for each applied load. One sphere is used for a series of four tests (5, 10, 15 and 20 min) and the sphere is slightly rotated after each test thereby creating a new circular mark around it at every test duration.

Additionally, corrosion tests were performed on nitrided and non-nitrided specimens in order to comparatively evaluate the electrochemical response of the systems. Experiments were made by means of potentiodynamic polarization tests. The electrochemical cell used to obtain the polarization curves applied a saturated calomel reference electrode and a platinum auxiliary electrode. The electrolyte employed was a Brazilian natural sea water with a pH of 8.0. Prior to the tests the system was led to rest for 10 min. For monitoring the potential and current, an *Autolab* model PGSTAT-302 potentiostat was applied. The polarization curves were obtained with a scanning speed of 1 mV/s from −1.0 to 1.0 V. For each experiment, 50 ml of the electrolyte was employed and the area exposed to the saline solution was approximately 0.5 cm^2. Each test was repeated twice and a representative curve is shown. It has been noticed that the error involved in the measurements, in terms of potential, may reach ± 50 mV.

Thus, wear and corrosion were evaluated after plasma nitriding at three different temperatures (450, 550 and 650 °C) and pressures (4, 5 and 6 mbar). Additionally, to further infer on the influence of the temperature cycle - solution treatment (1050 °C for 2 h), tempering (590 °C for 2 h) and nitriding (450, 550 or 650 °C for 5 h) - on the properties of the base steel, wear and corrosion tests were also performed on the back of the nitrided samples after metallographic preparation.

3. Results and interpretation

In the present study, the effect of nitriding temperature and pressure on the microstructure, wear and corrosion properties of the AISI H13 tool steel is addressed. Plasma nitriding has been successfully applied to several types of tool steels to improve fatigue [12], wear [13] and corrosion [7] properties. Processing parameters such as the method, gas mixture, nitriding temperature, time and pressure clearly influence the performance of a treated piece. Therefore the correct understanding on how these parameters affect the mechanical properties, composition, wear and corrosion is of prime importance to achieve a desirable response upon plasma nitriding of a specific alloy.

3.1. Microstructure and hardness

The microstructure of plasma nitrided AISI H13 was investigated by light optical microscopy and X-ray diffraction. The initial microstructure of the AISI H13 steel after austenitizing, quenching and tempering consists of martensite, primary carbides and secondary carbides which precipitated during tempering [3]. Upon nitriding the ingress of nitrogen promotes significant microstructural modifications in

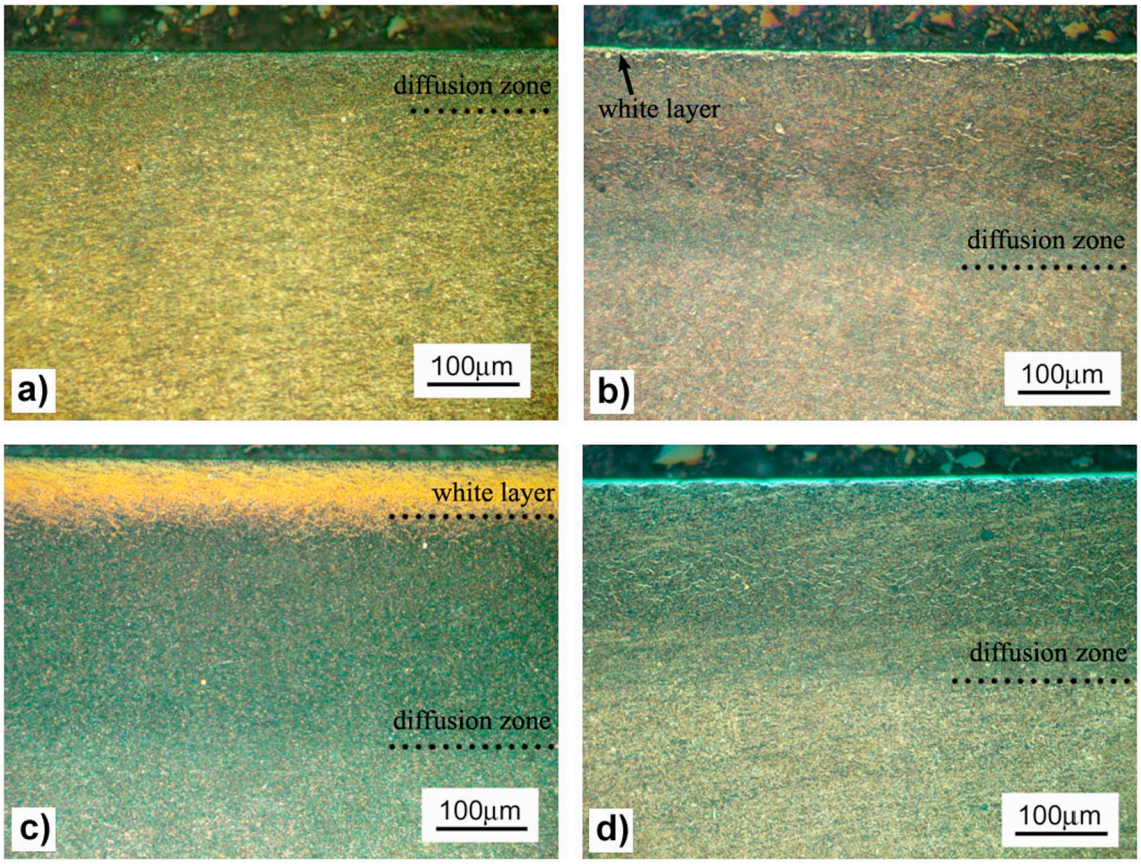

Fig. 1. Light optical micrographs from the cross sections of the AISI H13 steel plasma nitrided for 5 h at: (a) 450 °C and 5 mbar; (b) 550 °C and 5 mbar; (c) 650 °C and 5 mbar and (d) 550 °C and 6 mbar.

the near surface region. Moreover the applied nitriding treatment cycle (temperature and time) also leads to further microstructural alteration in the bulk acting as a second tempering step.

Fig. 1 presents a series of light optical micrographs from the cross sections of plasma nitrided AISI H13 at the same magnification. Fig. 1a shows a cross section of a specimen nitrided at 450 °C yielding only a surface diffusion zone. There is weak contrast between surface region and the core of the sample. Microhardness measurements were applied to confirm the transition between the diffusion zone and the inner core. Nitriding at 550 °C (Fig. 1b) results in a thin white surface layer plus a thick diffusion zone. In this case distinction between the diffusion zone and the substrate is clearer. Additionally, thin elongated precipitates are seen in the diffusion zone as a result of grain boundary precipitation [15,21]. At a temperature of 650 °C (Fig. 1c) the white surface layer is thicker and a deep diffusion zone is seen. Additionally, the white layer/diffusion zone interface is scattered indicating significant nitrogen diffusion across the grain boundaries. Fig. 1a to c was obtained from treatments applying 5 mbar of pressure.

Fig. 1d shows a cross section of a sample treated at 550 °C and 6 mbar allowing an evaluation of the influence of pressure on the layer morphology. Comparing Fig. 1b with Fig. 1d no clear difference is noticed indicating that pressure does not lead to significant morphological changes in the microstructure at the applied magnification.

Fig. 2 depicts plots of the nitrided case thickness against the applied temperature for different processing pressures. Case thickness includes the top white layer (when present) plus the diffusion zone. The plot indicates that case depth significantly increases as treatment temperature is raised. Meanwhile, the applied pressure appears to exert a minor influence.

Previous work indicates that a layer containing only a diffusion zone can be obtained by limiting the supply of nitrogen in the treatment

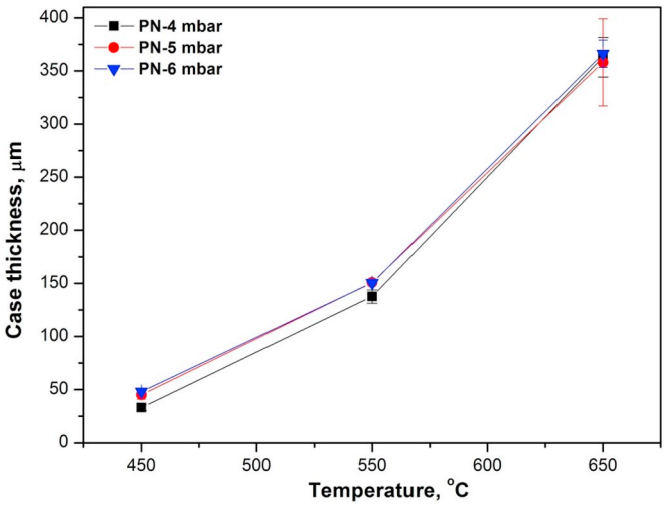

Fig. 2. A plot of the case thickness (µm) after plasma nitriding versus the applied temperatures for the three distinct pressures.

atmosphere [21]. In the present study such layer morphology was obtained at a temperature of 450 °C for 5 h of duration and for all the applied pressures. Higher treatment temperatures (550 and 650 °C) developed a white compound layer at the surface.

X-ray diffraction was applied to evaluate the nature of the compounds produced at surface of the steel after nitriding. Fig. 3 presents X-ray diffractograms from the plasma nitrided AISI H13 steel at 450 °C (Fig. 3a), 550 °C (Fig. 3b) and 650 °C (Fig. 3c). For a given temperature the layers produced at different pressures (i.e. 4, 5 and 6 mbar) are

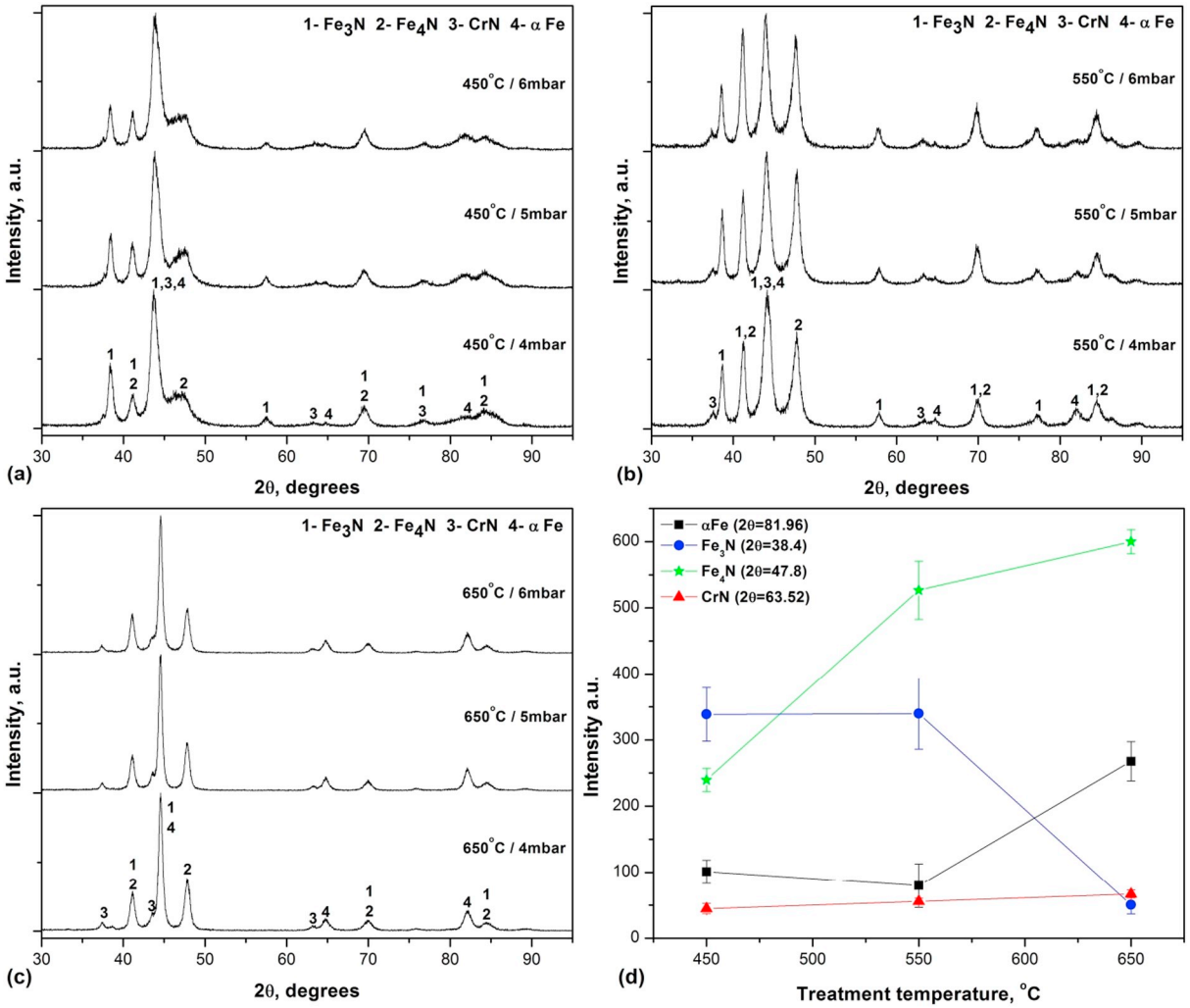

Fig. 3. X-ray diffractograms from the surface of the plasma nitrided AISI H13 samples produced at (a) 450 °C, (b) 550 °C, (c) 650 °C applying different processing pressures, and (d) qualitative phase evolution plot.

plotted as a stack. Additionally, a qualitative plot is given in Fig. 3d showing the variation in peak absolute intensity for selected phases. The results indicate that for a fixed temperature and time there is no significant effect of the applied pressure on the nature of the observed compounds (see Fig. 3a–c). However, the diffractograms are considerably distinct for the three applied temperatures.

Indeed as previously observed [5–7,22] the main phases produced after nitriding are the epsilon (ε-$Fe_{2-3}N$) and the gamma (γ′-Fe_4N) iron nitrides. Since AISI H13 steel has about 4 wt% of Cr, chromium nitride (CrN) is also observed, particularly for the treatments conducted at 550 and 650 °C. The observed diffraction peaks are generally broad at lower temperatures and become narrower at a higher temperature which is, to a certain extent, an indication of less disorder upon increasing process temperature [9].

The qualitative plot in Fig. 3d indicates that increasing the treatment temperature causes a decrease in the ε-nitride amount, as well as an increase in the γ′-nitride, CrN and α-Fe phase signal. According to Zagonel et al., for high plasma nitriding temperatures, the nitrogen diffusion from surface to the interior of the material is faster than the surface adsorption of nitrogen atoms from the plasma source, therefore yielding this phase distribution pattern [23].

Fig. 4 presents the microhardness profiles of plasma nitrided AISI H13 steel samples at the three different temperatures. Each hardness profile shows a superimposition of the data acquired for the three different applied pressures (i.e. 4, 5 and 6 mbar) at a constant treatment temperature. In fact there are no significant differences from the applied nitriding pressures in terms of hardness. All the profiles clearly show a high surface hardness, due to nitrogen ingress, which decreases towards the core of the specimen. Moreover, there is a clear decrease in

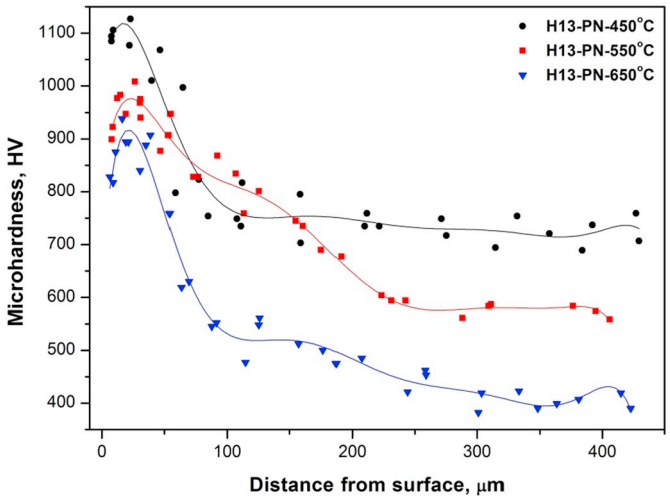

Fig. 4. Microhardness profiles of plasma nitrided H13 steel samples at different temperatures.

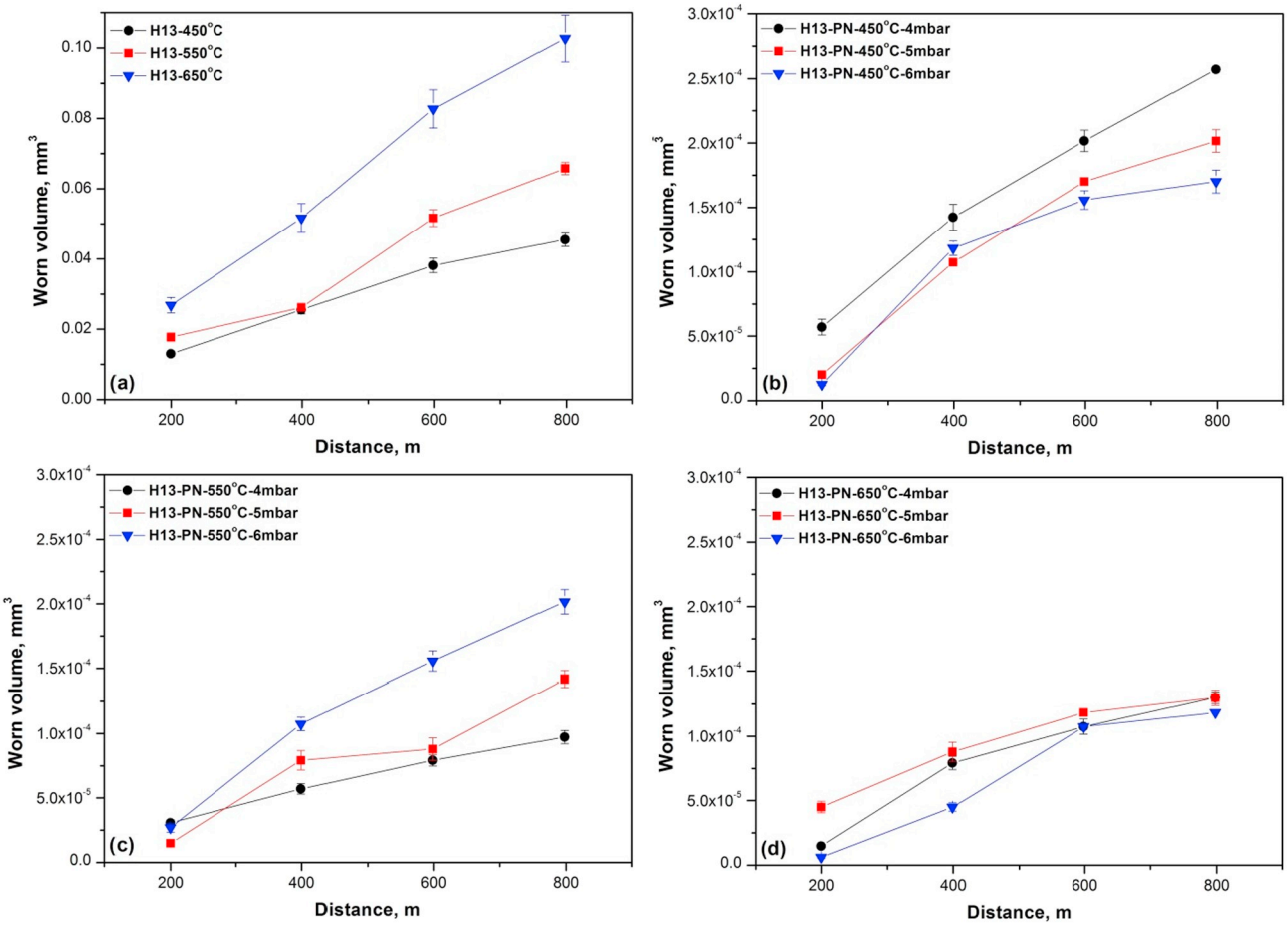

Fig. 5. Volume loss curves of the (a) tempered AISI H13 steel substrate and plasma nitrided samples at (b) 450 °C, (c) 550 °C and (d) 650 °C, applying different processing pressures.

both surface and core hardness when nitriding temperature is increased.

Plasma nitriding at 450 °C yields the highest surface hardness (about 1100 HV) and core hardness (nearly 720 HV). At 550 °C both the surface and core hardness decreases to 970 HV and 570 HV, respectively. Nitriding at 650 °C results in a further decrease in surface and core hardness to 900 HV and 400 HV, respectively. Previous studies have already shown that upon increasing the nitriding temperature maximum surface hardness diminishes [15,21].

The high surface hardness observed after nitriding is mainly attributed to the presence of iron nitrides (see Fig. 3) which are ceramic-like compounds. However, higher treatment temperatures appear to form coarser nitride precipitates leading to lower hardness within the case [24]. Additionally, the presence of porosity could also result in a decrease in hardness [17].

ASTM A681 advises that AISI H13 shall be tempered twice at 552 °C for a 2 h period which results in a minimum hardness of 52HRC (540 HV) [25]. In the present study tempering was performed once at 590 °C for 2 h resulting in a bulk hardness of 63HRC (770 HV). Plasma nitriding cycle would then act as a second tempering step. Previous microstructural investigations indicate that tempering twice at 650 °C results in a significant coarsening of carbides leading to a substantial loss in hardness [3]. Most likely the decrease in bulk hardness from the nitriding temperature of 450 to 650 °C (see Fig. 4) is related to such phenomenon.

Comparing case thickness exhibited in Fig. 2 with the hardness profiles from Fig. 4 it is noticed that case depth obtained from optical microscopy correlates reasonably well with the microhardness data. Samples treated at 450 °C exhibit a sudden drop in hardness while the specimens produced at 550 and 650 °C present a second hardness plateau beneath the surface.

3.2. Wear response

Fig. 5 presents dry wear test results conducted in the tempered AISI H13 steel substrate (Fig. 5a) and after plasma nitriding at 450 °C (Fig. 5b), 550 °C (Fig. 5c) and 650 °C (Fig. 5d) applying different working pressures. All curves show worn volumes increasing with the running distance. Note that different scales apply for the nitrided specimens and heat treated only readily indicating a considerable reduction in wear after nitriding.

Wear testing of the double tempered steel (standard tempering plus nitriding cycles) was conducted on the backside of the nitrided specimens therefore evaluating only the effect of heat treating on the tool steel. Tribological behaviors of tempered steel substrates (Fig. 5a) exhibit a direct relation with the observed bulk hardness. A larger worn volume is observed for the nitriding temperature of 650 °C which presented the lowest bulk hardness (see Fig. 4). Again, coarsening of carbides precipitated during the second tempering step (nitriding cycle) decreases hardness resulting in an impairment on the wear performance. Previous studies corroborate the reasoning [2].

Plasma nitriding yields an important improvement on the wear behavior, irrespective the processing temperature and pressure, with worn volumes 200 times smaller than the tempered steel. Analyzing Fig. 5b–d it is observed that for a treatment duration of 5 h temperature is the most significant parameter to generate reduction in the worn volume. Working pressure (from 4 to 6 mbar) appears to exert non-significant alterations in the volume lost since a clear trend could not be

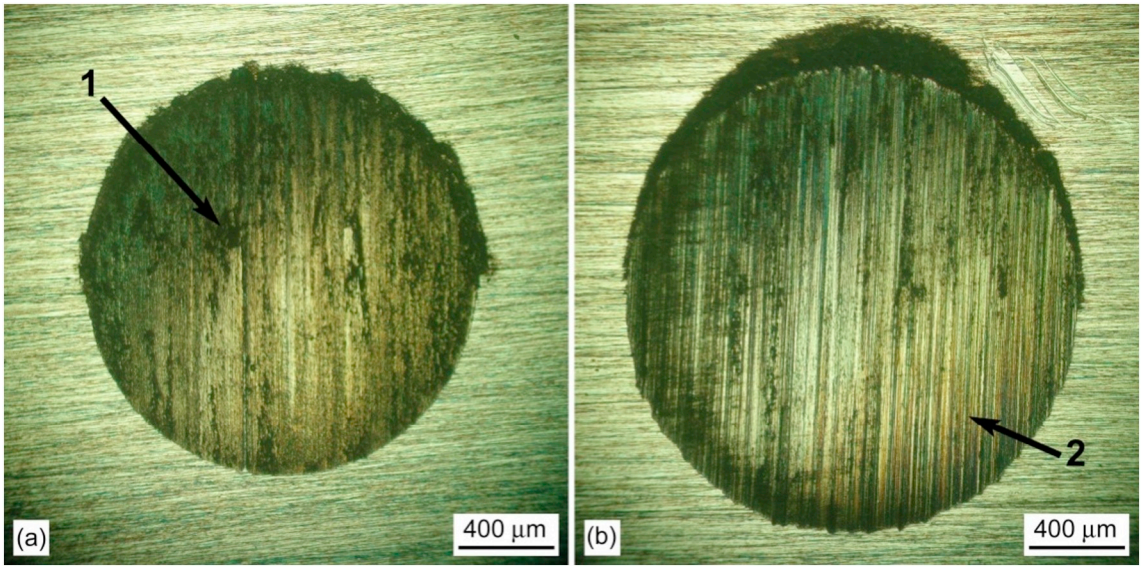

Fig. 6. Wear craters on the double tempered AISI H13 substrate. (a) 450 °C-5 h and (b) 650 °C-5 h, after 400 m of wear testing.

established. For the temperature of 650 °C, worn volumes are remarkably similar for the different applied pressures. However, for 450 and 550 °C there is a minor variation in wear depending on the pressure. In fact, increasing nitriding temperature appears to lead towards lowered worn volumes and a tendency of stabilization along the traveled distance. Plasma nitriding at 450 °C (Fig. 5b), which yielded higher surface hardness (see Fig. 4) results in increased worn volume.

With respect to the wear resistance several authors state that high hardness is a crucial parameter to maintain the surface integrity [13,26]. Notwithstanding the present results indicate the opposite for the nitrided specimens.

To further infer on the active wear mechanism during the wear tests in both tempered and nitrided steel samples, optical microscopy was conducted inside the wear craters. Fig. 6 shows micrographs from the wear tracks on the double tempered steel and Fig. 7 from the nitrided specimens. Wear craters from Fig. 6 correspond to wear testing with similar applied load and running distances after a second tempering step at 450 °C for 5 h (Fig. 6a) and 650 °C for 5 h (Fig. 6b), as a result from the nitriding cycle. Both micrographs show craters with parallel ridges (marked as 2) and adhesion patches (marked as 1) inside it, indicating a similar active wear mechanism. However, tempering at 650 °C (Fig. 6b) appears to yield deeper and wider ridges most likely as a result of its lower bulk hardness. Therefore material removal would be facilitated.

Although the tests were performed under dry condition, an abrasion wear mode is observed for all tempering conditions applied to the AISI H13 steel. Most likely, wear debris from the contact region generate a grooving process which yields such typical parallel scratches inside the wear craters.

The wear craters produced on the nitrided specimens (Fig. 7), applying the same testing conditions, are considerably smaller than those observed on the tempered steel (Fig. 6) as indicated by the scale bar on the images. In all cases the parallel scratches (marked as 2) generated inside the wear tracks are much less pronounced than those observed on the substrate, indicating a mild abrasive process.

Fig. 7a and b presents craters produced on the AISI H13 tool steel nitrided at 450 °C applying 5 mbar of pressure after 200 and 400 m of sliding, respectively. It is possible to see the size evolution and the development of wide dark adhesion areas (marked as 1) from 200 to 400 m of testing. As the wear process undergoes crater size tends to increase leading to a pressure decrease since load is constant. Lowering the pressure facilitates the entrance and entrapment of wear debris in the contact region causing the formation of such adhesion patches (marked as 1). Also, one notices the presence of wear debris on the superior part of all the produced scars.

Fig. 7c shows a crater produced after nitriding at 450 °C applying 4 mbar of pressure after 400 m of sliding. From Fig. 7b to c only pressure is modified from 5 to 4 mbar. Wear craters are very similar in size and morphology presenting regions of mild abrasion and adhesion.

On Fig. 7d and e wear scars from specimens nitrided at 550 °C applying 5 mbar of pressure after 200 and 800 m of sliding are shown, respectively. Both craters present the typical parallel scratches indicating an abrasive wear mode though mild in intensity due to the presence of shallow grooves.

Fig. 7f presents a wear scar on a specimen nitrided at 650 °C applying 4 mbar of pressure after 800 m of sliding. Plasma nitriding at this temperature yields the smallest craters and therefore the best wear performances (see Fig. 5). Again a mild abrasion process is noticed. Comparing Fig. 7e with Fig. 7f one notices the decrease in crater size by changing the nitriding temperature from 550 to 650 °C, respectively, for 800 m of sliding.

It is interesting to note that as nitriding temperature increases from 450 to 650 °C less adhesion patches are noticed inside the wear tracks (see Fig. 7) what could be attributed to a change in the contact nature leading a smaller work of adhesion [27]. At 450 °C nitriding results in a diffusion zone only and therefore the contact is mainly metal-metal in nature. At 650 °C a ceramic-like compound layer develops changing the contact nature to metal-ceramic thus decreasing the work of adhesion [27].

Another factor that might reduce the presence of adhesion patches inside the tracks is the size of the scar itself leading to pressure variation during sliding. Initially contact pressure is high and therefore wear debris are not allowed in the contact region. As sliding proceeds crater area increases leading to a decrease in the contact pressure. This allows debris entrapment which results in adhesion inside the wear tracks. Note that for nitriding at 650 °C adhesion is not observed even after 800 m of sliding (Fig. 7f) while for 450 °C after 400 m of sliding (Fig. 7b and c) adhesion is already present.

Table 1 collects the wear coefficients (K) and maximum crater depth (h) calculated from the worn volume curves previously presented in Fig. 5. Calculations based on the case thickness and crater depth indicate that wear tests performed on the plasma nitrided specimens have not perforated the nitrided layers even after 800 m of traveled distance (20 min of sliding).

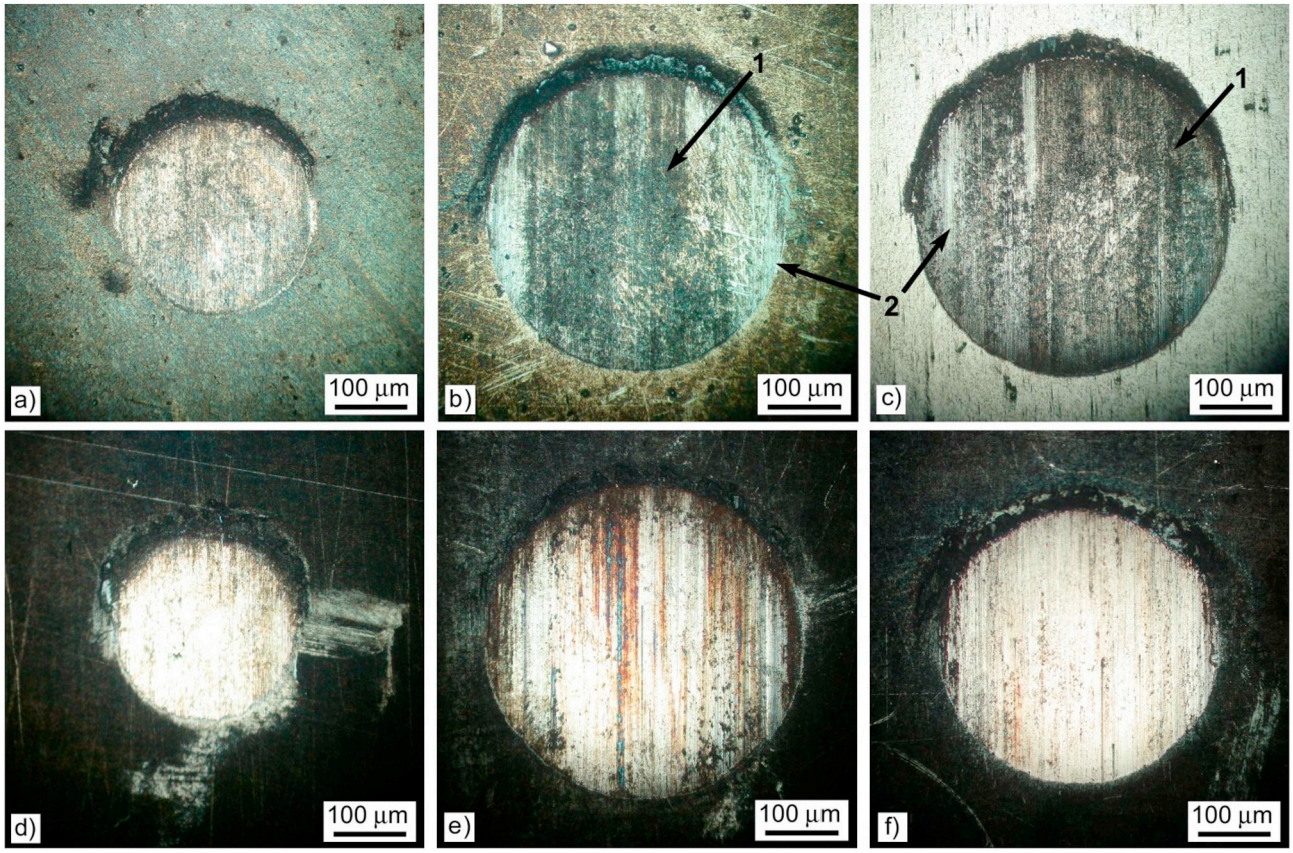

Fig. 7. Wear craters on the plasma nitrided AISI H13: (a) 450 °C-5 mbar-200 m, (b) 450 °C-5 mbar-400 m, (c) 450 °C-4 mbar-400 m (d) 550 °C-5 mbar-200 m, (e) 550 °C-5 mbar-800 m, (f) 650 °C-4 mbar-800 m.

Table 1
Wear coefficients (K) and crater depth (h) of the heat treated AISI H13 and plasma nitrided specimens.

		h, µm	K, $mm^3 \cdot m^{-1} \cdot N^{-1}$
450 °C	Substrate	33.8	$2.21 \cdot 10^{-5}$
	PN 4 mbar	2.54	$1.32 \cdot 10^{-7}$
	PN 5 mbar	2.25	$1.22 \cdot 10^{-7}$
	PN 6 mbar	2.07	$1.02 \cdot 10^{-7}$
550 °C	Substrate	40.6	$3.40 \cdot 10^{-5}$
	PN 4 mbar	1.56	$4.45 \cdot 10^{-8}$
	PN 5 mbar	1.89	$7.83 \cdot 10^{-8}$
	PN 6 mbar	2.24	$1.15 \cdot 10^{-7}$
650 °C	Substrate	50.7	$5.19 \cdot 10^{-5}$
	PN 4 mbar	1.80	$7.49 \cdot 10^{-8}$
	PN 5 mbar	1.80	$5.71 \cdot 10^{-8}$
	PN 6 mbar	1.72	$8.00 \cdot 10^{-8}$

Wear coefficients presented in Table 1 show an improvement of at least two orders of magnitude after plasma nitriding. Comparing the wear coefficients and crater depths of the tempered substrates it is clear that applying a second tempering at lower temperature yields better wear performances. Additionally, evaluating the effects of plasma nitriding alone, the specimens processed at 650 °C appear to possess higher wear resistances.

The wear coefficients from Table 1 are further plotted in function of nitriding temperature in Fig. 8a for comparison purposes. It depicts the wear coefficients of AISI H13 substrate, tempered at 450, 550 and 650 °C for 5 h, as a result of the temperature applied on the nitriding cycle. Additionally, an average of the wear coefficients from the nitrided specimens obtained at three different working pressures (i.e. 4, 5 and 6 mbar) is presented for each temperature. It is clear that tempering at higher temperatures leads to larger wear while nitriding at higher temperatures (for a fixed duration of 5 h) results in reduced wear.

Fig. 8b presents the evolution of adhesion percent, inside the wear craters, against the running distance after plasma nitriding at different temperatures as indicated. Each shadowed curve represents a nitriding temperature and the percent range in these shadowed areas indicates the maximum and minimum adhesion observed for the distinct applied pressures. The adhesion percent was obtained by analyzing the optical micrographs from the wear craters (see Fig. 7 for example) in which darker areas were accounted as regions of adhesion predominance.

Nitriding at lower temperatures (i.e. 450 °C) yields steadily increasing adhesion percent values that reach up to 65%. At 550 °C adhesion accounts for nearly 40% of the contact area after 800 m of wear testing while nitriding at 650 °C yield values as low as 15%. It is estimated that such dramatic variation in adhesion percent area, seen in Fig. 8b, is most likely related to the change in the contact nature as previously mentioned.

3.3. Electrochemical response

Tempered substrates and plasma nitrided samples were additionally submitted to corrosion testing in natural sea water. Fig. 9 presents potentiodynamic polarization tests conducted in the tempered AISI H13 steel substrate (Fig. 9a) and after plasma nitriding at 450 °C (Fig. 9b), 550 °C (Fig. 9c) and 650 °C (Fig. 9d) applying different working pressures. All curves are plotted with similar potential and current density scale ranges for comparison purposes. Table 2 summarizes the electrochemical parameters collected from the polarization curves presented in Fig. 9.

Fig. 9a indicates that after a second tempering step (in addition to the standard condition of 590 °C for 2 h), promoted by the plasma nitriding cycle (450, 550 or 650 °C for 5 h), corrosion properties of the

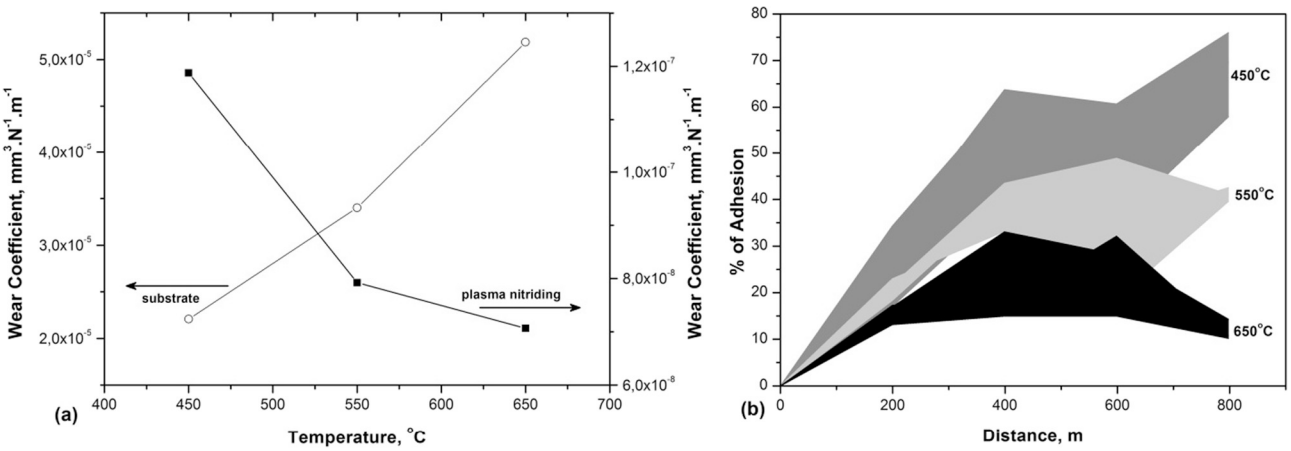

Fig. 8. (a) Wear coefficients of tempered AISI H13 steel substrate and plasma nitrided specimens, at different temperatures; and (b) evolution of the adhesion percent, inside the wear crater, of samples plasma nitrided at distinct temperatures.

bulk remain nearly unaltered irrespective the treatment temperature. The three applied temperatures result in very similar electrochemical behavior in which corrosion potentials are close and current density rises promptly without passivation. Corrosion potential is in the order of −700 mV as indicated by Table 2. After plasma nitriding at different temperatures and pressures very distinct electrochemical behaviors are observed.

Nitriding at 450 °C results in a considerable increase in the corrosion potential towards positive values and a decrease in current density for the three applied pressures (see Fig. 9b) when compared to the tempered steel substrate. Interestingly, this nitriding temperature yields the occurrence of multiple corrosion potentials, on the polarization curves, suggesting an unstable passive layer formation at the sample surface. Kelly et al, claim that when anodic and cathodic Evans lines intersect at three different points such multiple corrosion potentials occur [28]. Additionally, for the three applied pressures an

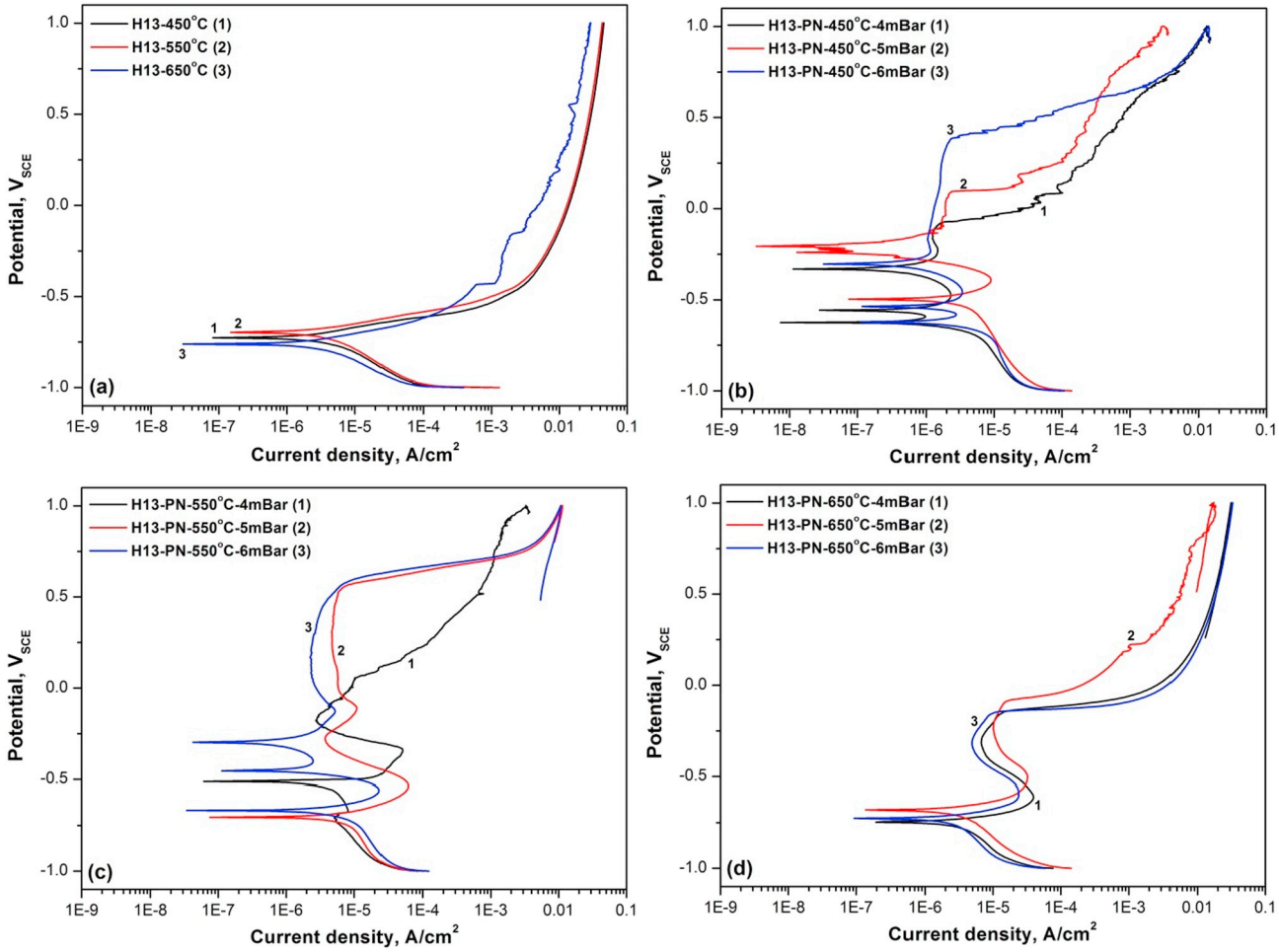

Fig. 9. Potentiodynamic polarization curves of (a) tempered AISI H13 steel and plasma nitrided at (b) 450 °C, (c) 550 °C and (d) 650 °C, applying different processing pressures.

Table 2
Electrochemical parameters from the polarization curves of plasma nitrided AISI H13.

Sample	E_{corr1}, mV	I_{corr1}, nA/cm^2	E_{corr2}, mV	I_{corr2}, nA/cm^2	E_{corr3}, mV	I_{corr3}, nA/cm^2	E_{pit}, mV
450-sub.	−727	81.18	–	–	–	–	–
450–4	−643	14.09	−558	52.89	−332	21.71	−81
450–5	−497	142.6	−240	24.65	−207	6.16	92
450–6	−622	207.9	−536	220.5	−304	59.31	367
550-sub.	−697	147.7					
550–4	−512	117.4	–	–	–	–	−164
550–5	−704	143.8	–	–	–	–	541
550–6	−667	65.73	−454	216.6	−298	81.58	535
650-sub.	−761	29.30	–	–	–	–	–
650–4	−746	373.9	–	–	–	–	−167
650–5	−680	264.1	–	–	–	–	−118
650–6	−725	178.4	–	–	–	–	−158

extensive passivation region is seen in which the current density remains small in magnitude. The extension of this passivation region appears to increase as pressure is raised from 4 to 6 mbar.

The electrochemical properties of samples plasma nitrided at 550 °C (Fig. 9c) also indicate an improvement when compared to the tempered substrate. Multiple corrosion potentials are observed only for the specimen treated at 6 mbar of pressure. Additionally, a wide passivation region is seen for samples produced at 5 and 6 mbar. Interestingly, plasma nitriding at 450 and 550 °C with 4 mbar of pressure yields a small passivation region (see Fig. 9b and c).

For nitriding at 650 °C the polarization curves (Fig. 9d) are relatively similar among all the three applied pressures. Corrosion potentials are in the same order of magnitude as those observed for the tempered substrate though current densities are somewhat larger (see Table 2). Additionally, the curves present a tentative of passivation with further abrupt increase of current density near the potential of -100 mV.

To further infer on the electrochemical behavior of the nitrided specimens the surface of corroded samples were analyzed with optical and electron microscopy. Fig. 10 presents micrographs of the whole corroded area (Fig. 10a, c and e) obtained with an optical microscope and magnified specific regions (Fig. 10b, d and f) captured with a scanning electron microscope. Changing nitriding temperature appears to influence significantly the surface morphology of the corroded specimens while altering working pressure from 4 to 6 mbar does not lead to relevant modifications.

Fig. 10a and b presents micrographs from the surface of a specimen nitrided at 450 °C with a pressure of 6 mbar and Fig. 10c and d shows images from a sample nitrided at 550 °C applying a pressure of 5 mbar, all after the exposure to the saline solution. Plasma nitriding at 450 and 550 °C yields similar morphology after polarization in which the surface exposed to the electrolyte appears to have suffered a generalized corrosion process with sparse pitting. The same characteristics are seen for the other applied pressures. During polarization, layers produced at 450 and 550 °C form a passivation film, and as applied potential increases, reaching the pitting potential, such film is broken and current density rises leading to localized corrosion as seen in Fig. 10b and d. The presence of corrosion pits could explain the shape of the polarization curves previously presented (Fig. 9b and c).

Plasma nitriding at 650 °C (irrespective the applied pressure) does not result in surface pitting after polarization. Fig. 10e and f depicts images from the surface morphology after polarization of a specimen nitrided at 650 °C with a pressure of 6 mbar. A different corrosion mechanism is noticed. It appears the electrolyte has promptly permeated through the top white compound layer (see Fig. 1c) developing corrosion residues beneath. The accumulation of residues builds an upward pressure that cracks the top white layer developing such a feature seen in Fig. 10f. Such mechanism was previously observed for other types of surface layers [29,30]. Most likely, nitriding at 650 °C develops a considerable amount porosity that allows the electrolyte to reach the diffusion zone beneath the top white layer.

From a general perspective the corrosion properties of the AISI H13 steel are influenced by plasma nitriding. Treatment temperature leads to more significant changes on the electrochemical response and corrosion morphology while applied pressure causes minor alterations.

3.4. Discussion

The present work addresses the influence of plasma nitriding applied to the AISI H13 tool steel. Effects of treatment temperature and pressure on the microstructure of the produced case, and additionally its wear and corrosion properties have been evaluated.

Previous studies indicate that typical microstructure of a nitrided tool steel consists of a top compound layer (white layer) followed by a nitrogen diffusion zone [5,6]. Optical micrographs presented in Fig. 1 show a similar morphology except for the layers produced at 450 °C which appear to yield only a diffusion zone. At this temperature the diffusivity of alloying elements is sluggish preventing a massive nitride precipitation [10]. The diffusion zone consists mainly of interstitial atoms in solid solution and fine, coherent nitride precipitates that are too small to be observed by optical microscopy [7]. At 550 and 650 °C of treatment temperature a thickening of this top white layer is observed and optical microscopy indicates a massive nitride formation at the surface, most likely due to faster diffusion. Previous work indicates that plasma nitriding at temperatures as low as 260 °C results in a considerably deep nitrogen diffusion zone [9].

For a fixed treatment time of 5 h case thickness significantly increases when temperature is raised from 450 to 650 °C, as indicated by Fig. 2. Changing the applied pressure does not lead to important modifications in terms of layer morphology and case thickness (see Figs. 1 and 2). Earlier studies have shown that at lower applied pressures a larger mean-free path develops which induces higher ion acceleration. This would enable nitrogen ions to diffuse deeper, therefore leading to thicker cases [10,31]. In the present work such tendency related to the applied pressure was not clearly observed due to the absence of a clear interface between the diffusion layer and the substrate which results in imprecise thickness measurements. However, the nature of the produced compounds and its relative fraction drastically change when nitriding temperature is increased.

X-ray diffraction analysis of plasma nitrided layers indicated very similar compounds, at a constant temperature and fixed treatment time (5 h), for the different applied pressures (4, 5 and 6 mbar) as seen in Fig. 3. Therefore, temperature appears to be the most significant parameter to induce nitride formation thus altering case morphology. Previous works also indicate that compound layer, which is the outermost surface layer, usually consists of iron nitrides such as ε-$Fe_{2-3}N$, γ′-Fe_4N, or a mixture of these phases [5–7]. At 450 °C, when only a diffusion zone is observed, ε-nitride is the major observed phase though γ′-nitride is also detected. Raising temperature to 550 °C leads to an increase in the γ′-nitride fraction while ε-nitride amount is maintained. Further increase in temperature to 650 °C nearly extinguishes the occurrence of the ε-nitride and γ′-nitride relative fraction continues to rise.

According to previous work, the mechanism of plasma nitriding involves an early formation of Fe_2N at the surface and its further decomposition to γ′-nitride or ε-nitride depending on the temperature [32]. At a lower temperature, which is likely the case for 450 °C, it is believed that nitrides are mainly formed as very fine particles preferentially at the grain boundaries. At higher temperatures diffusion into the material is fast enough to cause nitrogen depletion at the surface [9,23] thus leading to coarse precipitates and ultimately a thick white layer. Additionally, carbon content and alloying elements present in the steel play an important role in favoring the formation of the ε-phase [24]. Alloying elements such as Al, Cr, V for example, usually

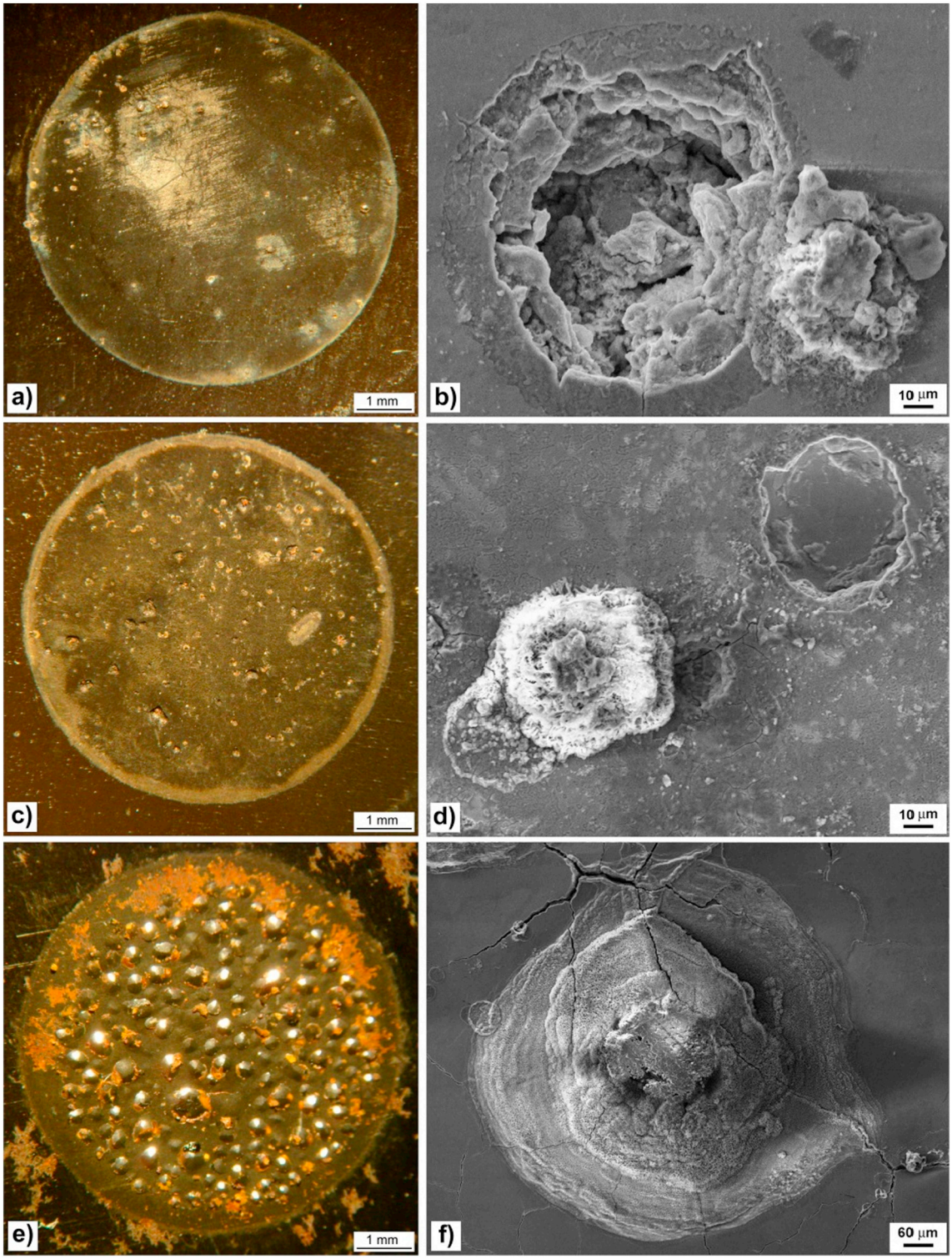

Fig. 10. Surface morphology after polarization tests obtained by optical (a, c, e) and electron microscopy (b, d, f) of AISI H13 steel nitrided at 450 °C (a, b), 550 °C (c, d) and 650 °C (e, f).

increase the nitrogen uptake ability of the steel.

Interestingly, the fraction of αFe phase also increases with temperature (see Fig. 3d). According to the literature, at higher temperatures nitrogen diffusion from surface to the bulk is faster than its adsorption to the surface which results in the presence of this phase [23]. Moreover, CrN precipitation slightly increases as treatment temperature is raised. Previous studies have already shown that plasma nitriding at 550 °C or above results in CrN phase in addition to the iron nitrides [21].

As a consequence of the production of ceramic-like compounds during nitriding a remarkable increase in the hardness of surface region is observed resulting in the profiles seen in Fig. 4. Again, the applied pressure appears to not influence significantly the hardness of the layers. When nitriding temperature is increased from 450 to 650 °C a significant loss of surface hardness is observed. Additionally, core hardness also decreases when treatment temperature is increased.

Above the secondary hardening peak temperature, fine carbides coarsen progressively and a strong reduction of the dislocation density occurs leading to a decrease in bulk hardness [2]. Karamiş found that for nitriding of AISI H13, longer treatment times and higher temperatures, both lead to lower surface hardness. The author attributes the decrease in hardness to the precipitation of coarse nitrides at higher temperatures [21].

Several authors point towards a direct correlation of hardness and wear resistance [14,33], according to the Archard's law [34]. In the present work such direct correlation was only observed for the base steel as a result of tempering in different conditions (see Fig. 5a). As previously stated bulk hardness decreases as nitriding temperature is increased as a result of carbide coarsening. Carbide coarsening at higher temperatures (e.g. 650 °C) affects the impact toughness and fracture resistance of the steel [2]. Dislocation rearrangement and annihilation is another phenomenon that is likely to influence the wear performance of tempered tool steels [3]. Wei et al, 2011, found similar results after tempering the AISI H13 steel at different temperatures for 2 h applying a pin-on-disc wear tester [2].

For plasma nitrided specimens a direct correlation between hardness and wear resistance is absent. In fact, an inverse correlation is observed. Plasma nitriding at lower temperatures (i.e. 450 °C) which yields higher surface hardness results in a slightly inferior wear resistance. Meanwhile, nitriding at 650 °C, irrespective the working pressure, yields better wear performance (see Figs. 5 and 8a).

Wear behavior of a given material is affected by several parameters. Examples include the applied load, ambient temperature, sliding velocity and ultimately the microstructure of the material [3]. Most of the tribological studies of nitrided AISI H13 employ a pin-on-disc type wear tester [14,26,33,35]. This configuration implies a pure sliding contact with an intermittent contact between the treated surface and the pin. In the present wear testing device a reference sphere rotates in a fixed point of a plasma nitrided surface leading to significant differences between the tests [20,36].

During pin-on-disc testing a contact point in a treated surface experiences a cyclic loading which does not occur in the micro-abrasive wear testing applied here. Therefore it is believed that test configuration is another parameter that might influence the results.

Karamiş has plasma nitrided the AISI H13 steel at 550 °C and found that wear rates are larger for longer treatment times (100 h) than for shorter ones (4 h). The author states that thicker compound layers include some pores and are more brittle. The observation is also valid for the variable temperature [7,15].

As previously mentioned, altering the working pressure did not result in significant case thickness, phase proportion or hardness changes after plasma nitriding. Therefore, it appears reasonable to expect similar worn volumes for the different applied pressures, at a fixed temperature, since these characteristics might dictate the wear behavior. Results from Fig. 5 and Table 1 indeed indicate that nitriding pressure does not exert significant changes in the tribological performance of the plasma nitrided AISI H13. Ramos et al, 2019, have plasma nitrided a microalloyed steel at different pressures and temperatures suggesting that treatments performed at higher pressures and temperatures yield better wear resistances [37]. Few papers in the literature address the influence of pressure on the wear performance of nitrided steels. Therefore further studies are necessary to unravel this matter.

A previous work found that the presence of a white layer, during nitriding of AISI H13, leads to a lower friction coefficient when compared to a diffusion zone only [14]. Also, the work of adhesion is significantly smaller in a metal-ceramic contact when compared to a metal-metal mating pair [27]. These findings corroborate the adhesion evolution presented in Fig. 8b which shows that nitriding at higher temperatures yields less adhesion during wear testing. Nitriding at 450 °C yields a nitrogen diffusion zone and therefore a metal-metal contact further resulting in a higher adhesion. Meanwhile, nitriding at 650 °C produces a top ceramic-like compound yielding a ceramic-metal contact which results in lower adhesion.

Different types of thermochemical treatments have been historically applied to enhance the corrosion resistance of ferrous alloys. Diffusion of nitrogen and/or carbon are among the most common ones. It is believed that producing iron nitrides, for example, at the surface changes its nature towards a more stable compound and therefore improves the electrochemical properties. However, the type and morphology of this iron compound is important as well.

Polarization experiments, applied to evaluate the corrosion properties of tempered only and plasma nitrided AISI H13, suggest that nitrogen ingress is an efficient way of improving the electrochemical response of a tool steel. However, plasma processing conditions, especially temperature, must be carefully selected in order to yield adequate properties. Several authors have already demonstrated the effect of nitrogen on the corrosion behavior of ferrous alloys, including the AISI H13 steel [7,38,39]. When correctly applied, nitrogen diffusion appears to develop a wide passivation region in the AISI H13 tool steel therefore improving its corrosion resistance as indicated by Fig. 9b and c. It has been suggested that nitrogen reacts with H^+ in the solution leading to higher pH values therefore preventing the progress of corrosion [40].

Since nitriding was applied at a range of temperatures from 450 to 650 °C the temperature cycle applied by the thermochemical treatment acts as a second tempering step on the tool steel, in addition to the standard cycle (590 °C for 2 h). As presented by Fig. 9a and Table 2 altering the tempering temperature has not led to significant changes on the corrosion behavior of the steel.

Plasma nitriding the AISI H13 steel at 450 and 550 °C results in extended passivity, higher corrosion potentials and reduced corrosion current densities (see Table 2). For these temperatures a passive film is likely formed which is later disrupted by the increase on the applied potential thus leading to localized corrosion (see Fig. 10b and d). Previous studies confirm the corrosion morphology after polarization in a saline solution [7,41]. Nitriding pressure appears to influence the shape of the polarization curve. However, further studies are necessary to confirm it.

Increasing nitriding temperature to 650 °C seems to significantly decrease the observed passivation extent irrespective the applied pressure (see Fig. 9d). Also, the observed corrosion potentials and current densities are somewhat similar to those from the tempered only steel. Interestingly, the surface aspect after polarization indicates a distinct mechanism in which the electrolyte permeates through the nitrided layer.

Previous works have already shown that during polarization at high applied potentials the electrolyte appears to permeate through the layer reaching the base alloy. The dissolution of the base alloy would lead to an upward pressure build up [29]. In the present study the layers produced at 650 °C clearly exhibit a similar corrosion mechanism (see Fig. 10e and f). Such mechanism is possible due to the development of porosity during plasma nitriding. Porosity appears to develop as a consequence of the instability of iron nitrides which decomposes in pure iron and nitrogen gas [16,17,42]. Most likely the porosity development is more favorable for longer nitriding times and higher temperatures.

Earlier studies claim that ε-nitride is more corrosion resistant than the γ′-nitride [7]. Therefore, the loss in corrosion resistance and passivation ability observed for the specimens produced at 650 °C could be related to the depletion of this phase in the layer. Another fact that is likely to contribute to the loss in corrosion resistance is the presence of porosity as previously suggested [43].

Another curious observation is the occurrence of multiple corrosion potentials after nitriding at 450 °C with 4, 5, and 6 mbar of pressure and at 550 °C with 6 mbar. Previous work has found that the number of the corrosion potentials is influenced by the acid concentration and oxygen content in the solution [44]. Recently, Li et al. showed that scanning rate also might affect the observation of multiple corrosion potentials

[45].

From the wear and corrosion perspective the present results indicate that plasma nitriding of AISI H13 at 450 or 550 °C leads to better corrosion properties while nitriding at 650 °C yields a better wear performance. Therefore, in circumstances such as polymer processing by injection molding, for example, low temperature nitriding could be more adequate. And, in a forging operation were different types of wear mechanisms operate plasma nitriding at higher temperatures appears to be the correct choice.

4. Summary

Plasma nitriding of tempered AISI H13 tool steel leads to significant changes on the microstructure, wear and corrosion properties. Nitriding at a temperature of 450 °C yields a diffusion zone while at 550 or 650 °C produces a top compound layer at the surface. Both surface and bulk hardness decrease as nitriding temperature is increased. X-ray diffraction indicates that increasing the treatment temperature causes a decrease in the ε-nitride amount, as well as an increase in the γ′-nitride, CrN and α-Fe phase signal.

Altering the applied pressure does not yield significant changes in terms of microstructure, hardness and wear properties. Plasma nitriding leads to reductions of two orders of magnitude in the wear coefficients when comparing to the tempered steel. Wear resistance was found to increase as nitriding temperature is increased. Additionally, nitriding at higher temperatures appears to result in a reduction on the adhesion in the wear tracks.

Regarding the corrosion behavior, nitriding at 450 and 550 °C yields extended passivity, higher corrosion potentials and reduced corrosion current densities when comparing to the tempered only steel. Increasing nitriding temperature to 650 °C seems to significantly decrease the observed passivation extent irrespective the applied pressure.

CRediT author statement

F.A.P. Fernandes, wrote the manuscript and performed wear experiments.

S.C. Heck analyzed XRD results and performed wear experiments.

C.A. Picone performed electrochemical experiments and analyzed the results.

L.C. Casteletti supervised the work and conceptualized the experiments.

Declaration of competing interest

The authors declare that they have no known competing financial interests or personal relationships that could have appeared to influence the work reported in this paper.

Acknowledgments

The authors are grateful for the Brazilian funding agencies CAPES and CNPq.

References

[1] A. Eser, C. Broeckmann, C. Simsir, Comput. Mater. Sci. 113 (2016) 280–291.
[2] M.X. Wei, S.Q. Wang, L. Wang, X.H. Cui, K.M. Chen, Tribol. Int. 44 (2011) 898–905.
[3] A. Medvedeva, J. Bergström, S. Gunnarsson, J. Andersson, Mater. Sci. Eng. A 523 (2009) 39–46.
[4] K.-M. Winter, J. Kalucki, D. Koshel, Process technologies for thermochemical surface engineering, in: E.J. Mittemeijer, M.A.J. Somers (Eds.), Thermochemical Surface Engineering of Steels: Improving Materials Performance, 1st ed, Woodhead Publishing, 2014, pp. 141–206.
[5] S.D. Jacobsen, R. Hinrichs, I.J.R. Baumvol, G. Castellano, M.A.Z. Vasconcellos, Surf. Coat. Technol. 270 (2015) 266–271.
[6] S.D. Jacobsen, R. Hinrichs, C. Aguzzoli, C.A. Figueroa, I.J.R. Baumvol, M.A.Z. Vasconcellos, Surf. Coat. Technol. 286 (2016) 129–139.
[7] D.C. Wen, Appl. Surf. Sci. 256 (2009) 797–804.
[8] S.S. Hosmani, R.E. Schacherl, E.J. Mittemeijer, Acta Mater. 54 (2006) 2783–2792.
[9] L.F. Zagonel, C.A. Figueroa, R. Droppa Jr., F. Alvarez, Surf. Coat. Technol. 201 (2006) 452–457.
[10] G.F. Gomes, M. Ueda, H. Reuther, J. Appl. Phys. 94 (2003) 5379–5383.
[11] M. Naeem, Z.I. Khattak, M. Zaka-ul-Islam, S. Shabir, A.W. Khan, M. Zakaullah, Radiat. Eff. Defects Solids 169 (2014) 893–905.
[12] S.M.Y. Soleimani, A.R. Mashreghi, S.S. Ghasemi, M. Moshrefifar, Mater. Des. 35 (2012) 87–92.
[13] M.V. Leite, C.A. Figueroa, S. Corujeira Gallo, A.C. Rovani, R.L.O. Basso, P.R. Mei, I.J.R. Baumvol, A. Sinatora, Wear 269 (2010) 466–472.
[14] A. Mahmoudi, M. Esmailian, Adv. Mater. Res. 83-86 (2010) 41–48.
[15] M.B. Karamiş, Thin Solid Films 203 (1991) 49–60.
[16] M.B. Karamiş, Mater. Sci. Eng. A 168 (1993) 49–53.
[17] M.A.J. Somers, International Heat Treatment and Surface Engineering 5 (2011) 7–16.
[18] S.S. Akhtar, A.F.M. Arif, B.S. Yilbas, Gas nitriding of H13 tool steel used for extrusion dies: numerical and experimental investigation, in: M.S.J. Hashmi (Ed.), Comprehensive Materials Finishing, 3 2017, pp. 158–177.
[19] F.A.P. Fernandes, A. Lombardi Neto, L.C. Casteletti, A.M. de Oliveira, G.E. Totten, Heat Treating Progress 8 (2008) 41–43.
[20] C.K.N. Oliveira, R.M. Muñoz Riofano, L.C. Casteletti, Surf. Coat. Technol. 200 (2006) 5140–5144.
[21] M.B. Karamiş, Wear 150 (1991) 331–342.
[22] R.L.O. Basso, C.A. Figueroa, L.F. Zagonel, H.O. Pastore, D. Wisnivesky, F. Alvarez, Plasma Process. Polym. 4 (2007) S728–S731.
[23] L.F. Zagonel, R.L.O. Basso, F. Alvarez, Plasma Process. Polym. 4 (2007) S736–S740.
[24] M.B. Karamiş, Thin Solid Films 217 (1992) 38–47.
[25] "Standard Specification for Tool Steels Alloy", ASTM A681, ASTM, Philadelphia, PA, USA, 2015.
[26] G. Castro, A. Fernández-Vicente, J. Cid, Wear 263 (2007) 1375–1385.
[27] K.H. Zum-Gahr, Microstructure and Wear of Materials, 1st ed., Elsevier, 1987.
[28] R.G. Kelly, J.R. Scully, D.W. Shoesmith, R.G. Buchheit, Electrochemical Techniques in Corrosion Science and Engineering, 1st ed., CRC Press, 2002.
[29] Y. Sun, Corros. Sci. 52 (2010) 2661–2670.
[30] F.A.P. Fernandes, J. Gallego, C.A. Picon, G. Tremiliosi Filho, L.C. Casteletti, Surf. Coat. Technol. 279 (2015) 112–117.
[31] A. Nishimoto, K. Nagatsuka, R. Narita, H. Nii, K. Akamatsu, J. ASTM Int. 8 (2011) 1–7.
[32] E. Metin, O.T. Inal, J. Mater. Sci. 22 (1987) 2783–2788.
[33] A.R. Mashreghi, S.M.Y. Soleimani, S. Saberifar, Mater. Des. 46 (2013) 532–538.
[34] J.F. Archard, J. Appl. Phys. 24 (1953) 981–988.
[35] B. Wang, X. Zhao, W. Li, M. Qin, J. Gu, Appl. Surf. Sci. 431 (2018) 39–43.
[36] F.A.P. Fernandes, S.C. Heck, R.G. Pereira, C.A. Picon, P.A.P. Nascente, L.C. Casteletti, Surf. Coat. Technol. 204 (2010) 3087–3090.
[37] H.E.L. Ramos, A.R. Franco Jr., E.A. Vieira, J. Mater. Res. Technol. 8 (2019) 1694–1700.
[38] L.L.G. da Silva, M. Ueda, R.Z. Nakazato, Surf. Coat. Technol. 201 (2007) 8291–8294.
[39] Z.A. Fazel, H. Elmkhah, M. Nouri, A. Fattah-Alhosseini, Materials Research Express 6 (2019) 056412.
[40] R.F.A. Jargelius-Pettersson, Corros. Sci. 41 (1999) 1639–1664.
[41] R.L.O. Basso, H.O. Pastore, V. Schmidt, I.J.R. Baumvol, S.A.C. Abarca, F.S. de Souza, A. Spinelli, C.A. Figueroa, C. Giacomelli, Corros. Sci. 52 (2010) 3133–3139.
[42] M.A.J. Somers, E.J. Mittemeijer, Metall. Mater. Trans. A 26 (1995) 57–74.
[43] R.L.O. Basso, R.J. Candal, C.A. Figueroa, D. Wisnivesky, F. Alvarez, Surf. Coat. Technol. 203 (2009) 1293–1297.
[44] Y.X. Qiao, Y.G. Zheng, P.C. Okafor, W. Ke, Electrochim. Acta 54 (2009) 2298–2304.
[45] Y.J. Li, Y.G. Wang, B. An, H. Xu, Y. Liu, L.C. Zhang, H.Y. Ma, W.M. Wang, PLoS One 11 (1) (2016) e0146421, , https://doi.org/10.1371/journal.pone.0146421.